Journal of Alloys and Compounds 488 (2009) 227–231

Contents lists available at ScienceDirect

Journal of Alloys and Compounds

journal homepage: www.elsevier.com/locate/jallcom

Influence of stirring velocity on the synthesis of magnetite nanoparticles (Fe_3O_4) by the co-precipitation method

Roberto Valenzuela[a], María Cecilia Fuentes[a], Carolina Parra[a], Jaime Baeza[b], Nelson Duran[c], S.K. Sharma[d], Marcelo Knobel[d], Juanita Freer[b,*]

[a] Renewable Resources Laboratory, Biotechnology Center, Universidad de Concepción, Casilla, 160-C, Chile
[b] Faculty of Chemical Sciences, Universidad de Concepción, Casilla, 160-C, Chile
[c] Biological Chemistry Laboratory, Chemistry Institute, Universidade Estadual de Campinas, CP 6154 Campinas, SP – CEP 13083-970, Brazil
[d] Low Temperatures Materials Laboratory, Physics Institute, Universidade Estadual de Campinas, CP 6165 Campinas, SP – CEP 13083-970, Brazil

ARTICLE INFO

Article history:
Received 29 April 2009
Received in revised form 20 August 2009
Accepted 20 August 2009
Available online 27 August 2009

Keywords:
Oxide materials
Nanofabrication
Structure
Magnetic measurements

ABSTRACT

Superparamagnetic magnetite nanoparticles (mean diameter ~10 nm) were synthesized using the co-precipitation route from Fe^{2+}/Fe^{3+} in aqueous solutions (molar ratio 1:2) by adding a base under mechanical stirring at 10,000 rpm. This stirring velocity was found to be suitable for obtaining nanoparticles of this mean size, and a decrease in stirring velocity resulted in a larger size (~19 nm) and a wider size distribution. At 18,000 rpm, in addition to magnetite, goethite is also synthesized in the form of nanoparticles and nanorods are found. At higher stirring velocities (25,000 rpm), the solution's core temperature increased from 20° to 37 °C, generating a mixture of non-magnetic iron compounds.

1. Introduction

Synthetic iron oxide magnetite (Fe_3O_4) nanoparticles have been widely studied in the last decades, and an increasing number of scientific and technological applications have been developed, such as: solid support for enzymes such as cellulase [1], glucose oxidase [2], bovine serum albumin [3] homing peptides [4] and lipase [5]; magnetite bounded to chitosan acts as a nano-absorbant for the removal of heavy metals [6]; and when using a highly active heterogeneous Fenton system based on iron metal and magnetite, Fe^0/Fe_3O_4 has been used to oxidize synthetic dyes [7]. It also has been used in biomedicine as a magnetic drug delivery system (MDDS) [8–10], as a contrast agent for magnetic resonance imaging (MRI) [11,12] and as heating mediator for cancer thermotherapy [13,14]. Magnetite remains as the only magnetic nanoparticle (MNP) approved for clinical use to date [15] because it features low toxicity effects in cells [16]. It has also been used to make conductimetric immunosensors for *E. coli* detection [17].

Numerous and diverse methodologies exist to synthesize magnetic nanoparticles of magnetite in order to obtain different shapes (microspheres, nanospheres, nanorods and ferrofluids), sizes and with high saturation magnetization (M_s), including oxidation with H_2O_2 of a suspension of $Fe(OH)_2$ [2,18,19], reduction of hematite by CO/CO_2 [20], flame spray synthesis [21], microemulsion technology [22] and thermal decomposition of iron pentacarbonyl [23] or iron (III) acetylacetonate in tri(ethyleneglycol) [24]. However, the most common method for producing synthetic magnetite nanoparticles is the co-precipitation of Fe^{2+}/Fe^{3+} ions (molar ratio 1:2) by alkaline solutions [6,25,26], reacting as indicated in the equation below. This method generally produces particles with diameters of 10 nm or less.

$$Fe^{2+} + 2Fe^{3+} + 8OH^- \rightarrow Fe_3O_4 + 4H_2O \quad (1)$$

Although this method to prepare magnetite nanoparticles is well known, some difficulties still exist due to limited control of the synthesis process used to obtain pure magnetite with proper size distribution, shape and morphology. The concentration, molar ratio of the reactants, pH and temperature are some of the important factors to control phase and size [27–29].

This work studied the influence of the stirring velocity on the particle size of the magnetite nanoparticles synthesized by the co-precipitation method because the dispersed phase should be largely distributed in a uniform manner over the entire liquid height for crystallization and solid catalyzed reactions, a condition that requires both higher stirring speeds and power [30]. Also as the stirrer speed increases, the reaction solution's uniformity improves and smaller particles and narrower size distributions are obtained [30–32].

* Corresponding author. Tel.: +56 41 2207295; fax: +56 41 2207440.
E-mail address: jfreer@udec.cl (J. Freer).

0925-8388/$ – see front matter © 2009 Elsevier B.V. All rights reserved.
doi:10.1016/j.jallcom.2009.08.087

Table 1
Temperature control of the solutions under different stirring velocities.

Stirring velocities	T_{In} (°C)	T_{Fin} (°C)
Magnetic stirring	20.0 ± 0.5	20.0 ± 1.0
10 000 rpm	20.0 ± 0.5	21.0 ± 1.7
18 000 rpm	20.0 ± 0.5	22.7 ± 0.5
25 000 rpm	20.0 ± 0.5	37.3 ± 1.5

2. Experimental

2.1. Materials

All reagents were pro-analysis and used as received without further purification. $FeSO_4{\cdot}7H_2O$, $FeCl_3{\cdot}6H_2O$ and ammonia 25 wt.% were purchased from Merck. Nanopure water (NPW) was used in all the preparations.

2.2. Synthesis of magnetite nanoparticles

Magnetite nanoparticles were synthesized using the co-precipitation method. 300 mL of a 0.05 M $FeSO_4{\cdot}7H_2O$ and 0.1 M $FeCl_3{\cdot}6H_2O$ solution was poured in a beaker, deoxygenated for 30 min with N_2(g) and the solution's temperature was maintained at 20 °C (T_{In}). Ammonia was added into the solution at a constant rate of 35 mL/min using a peristaltic pump in order to reach pH 10 in 2 min under constant stirring. The solution's final temperature was measured (T_{Fin}). The stirring velocities tested to co-precipitate the Fe^{2+}/Fe^{3+} ions by ammonia were: vigorous magnetic stirring (MNP-MS), 10,000 rpm (MNP-10 000), 18,000 rpm (MNP-18 000) and 25,000 rpm (MNP-25 000). The last three stirring velocities were obtained using a D-500 Wiggen Hauser Homogenizer with an ER_{20} rotor/$S_{20}F$ stator system. The suspensions obtained were aged and digested at 80 °C for 30 min under a gentle magnetic stirring [33] and cooled at room temperature. Magnetic nanoparticles were magnetically separated while non-magnetic nanoparticles were harvested by centrifugation. To purify the products, the samples were washed repeatedly with NPW and ethanol until pH 7. The particles were then dried at 74 °C overnight under vacuum.

2.3. Characterization

The samples' crystal structure were analyzed by X-ray diffraction (XRD) with a Rigaku D/Max-C model diffractometer using Fe Kα radiations (λ = 1.93 Å). To confirm the synthesis of magnetite rather than maghemite (γ-Fe_2O_3), which has an identical XRD diffraction pattern, XPS was used to examine the Fe:O stoichiometry. The XPS data were obtained with a ESCALAB 220i-XL (VG Scientific) instrument using a monochromated Al Kα X-rays source for sample excitation. High quality depth profiles were obtained with an EX05 (VG Scientific) ion gun. Low ion energy was used to maximize depth resolution. The base pressure was better than 5×10^{-9} mbar. The data was collected with a microprocessor interfaced to a PC computer. The VG-Eclipse v2.1 data system processed the XPS data. Low-resolution survey spectra were first acquired to identify the various surface elements. Each element concentration was then calculated from the area of the corresponding peak in a high-resolution spectrum, which is the area of a Gaussian-Lorentzian line fitted to the high-resolution peak after subtraction of background noise. The size distribution, shape and morphology of the magnetite nanoparticles were determined using transmission electron microscopy (TEM). The images were taken using a JEOL JEM 1200EXII microscope at an accelerating voltage of 120 kV. The samples were re-dispersed in a NPW/ethanol (1:1) matrix, and then deposited on a 200-mesh carbon-nitrocellulose coated TEM copper grid. To determine the size distribution and the mean average size, 100 particles were measured for each sample. The hydrodynamic diameter for the dispersed samples was determined by dynamic light scatter (DLS) using a Malvern Nano Zeta Sizer at 25 °C. The samples' magnetic properties were analyzed using a MPMS superconducting quantum interference device (SQUID) magnetometer from Quantum Design, XL model at 300 K in an applied field ±20 kOe.

3. Results and discussion

High velocity stirring during the preparation of magnetite nanoparticles produces a temperature increase in the Fe^{2+}/Fe^{3+} solution (Table 1). This increase in temperature is considerable at 25,000 rpm, producing a non-magnetic brown red suspension of iron compounds instead of the dark brown suspension characteristic of magnetite.

Fig. 1 displays the XRD pattern of the prepared samples at different stirring velocities. The diffraction peaks for the samples MNP-MS and MNP-10 000 (Fig. 1(a) and (b)) can be indexed to cubic phase of magnetite without any secondary phase. The peak

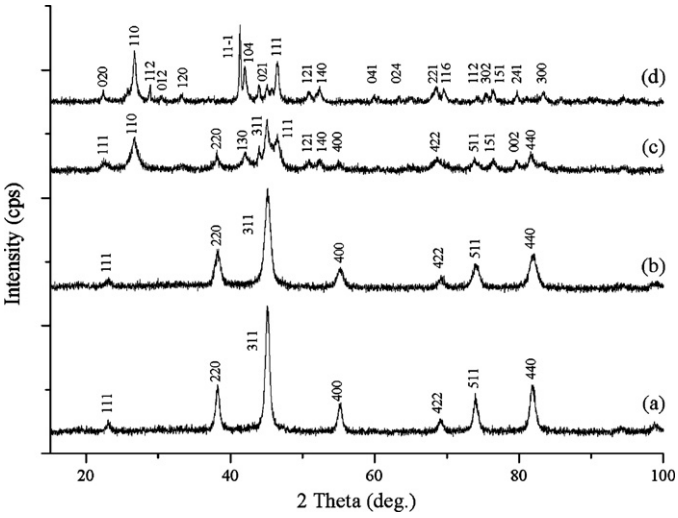

Fig. 1. XRD patterns for the samples (a) MNP-MS, (b) MNP-10 000, (c) MNP-18 000 and (d) MNP-25 000.

positions and corresponding Miller indexes match well with the values reported for the bulk materials (JCPDS file no. 85–1436). However, the XRD analysis for the MNP-18 000 sample (Fig. 1 (c)) reveals that in addition to the cubic phase of magnetite (JCPDS file no. 19–0629), goethite with an orthorhombic phase (JCPDS file no. 29–0713) is also found. On the other hand, the XRD analysis of the MNP-25 000 sample (Fig. 1 (d)) shows the formation of a brown non-magnetic powder that consists in a mixture of hematite, goethite and iron-oxide (JCPDS files no. 86–0550, 81–0463 and 76–1821, respectively). The increase in the solutions' core temperature during synthesis by co-precipitation initially promotes the partial thermal transformation of magnetite to goethite [34], and then the dehydroxylation of goethite forms the amorphous Fe_2O_3

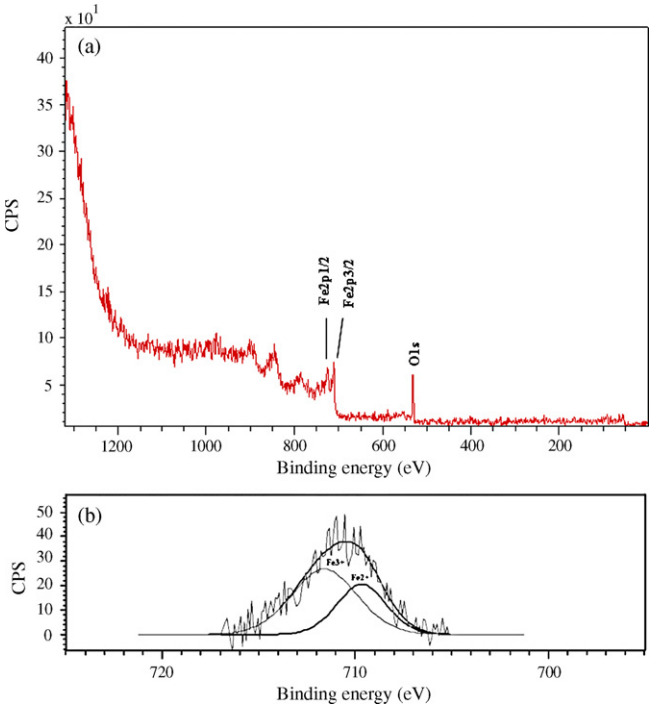

Fig. 2. XPS spectra for the magnetite sample: (a) entire energy range; (b) Deconvultion of the Fe $2p_{3/2}$ peak.

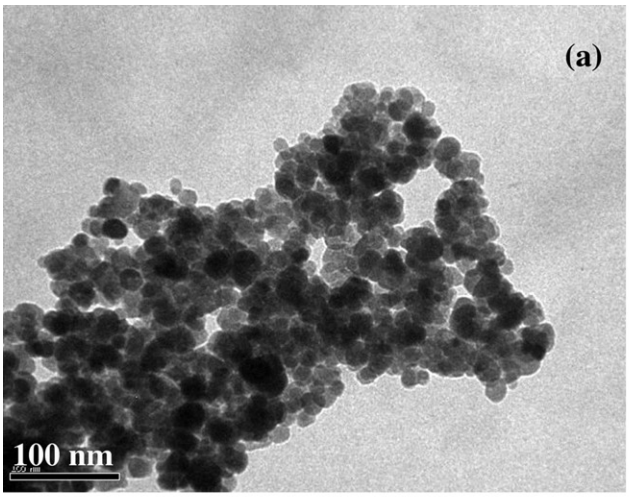

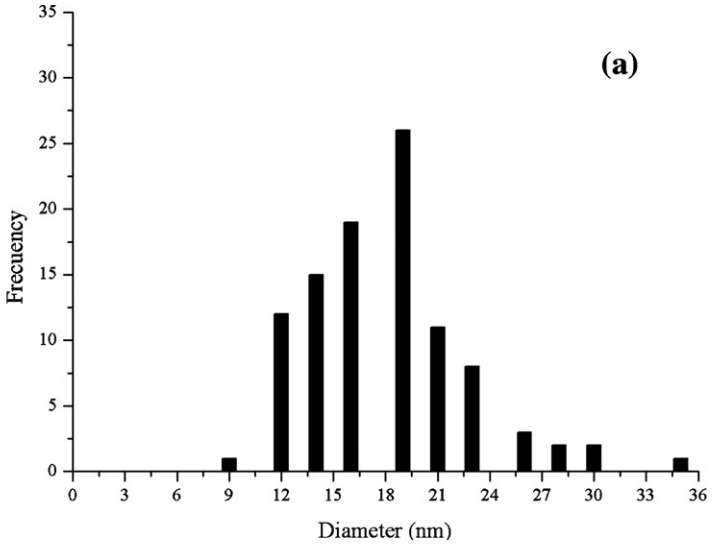

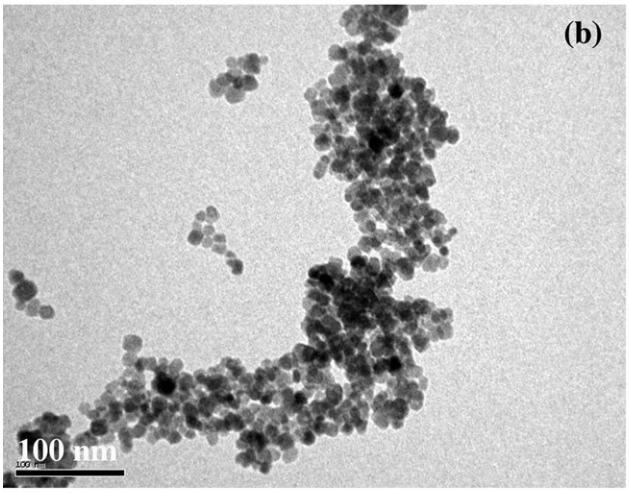

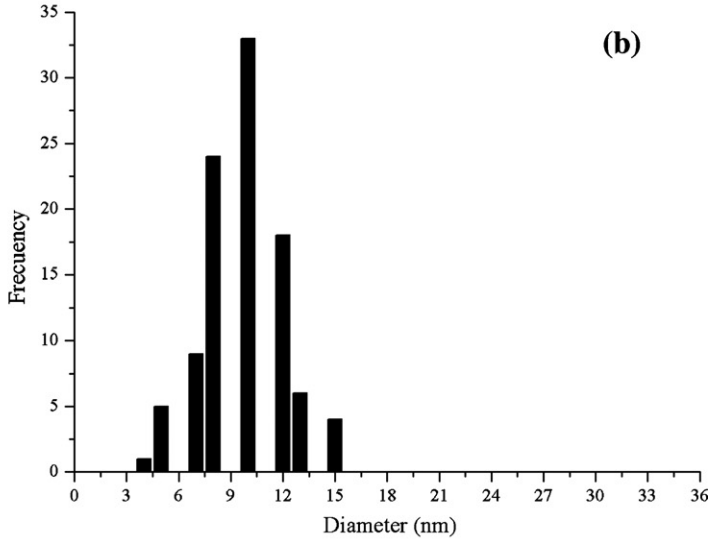

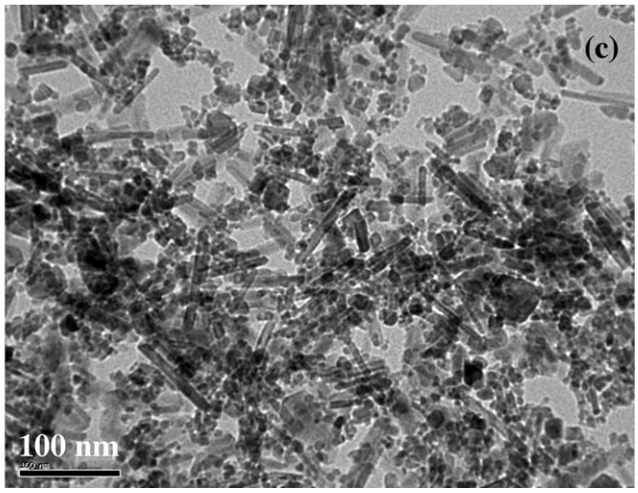

Fig. 3. TEM images and diameter distributions for samples with stirring velocities of (a) MNP-MS, (b) MNP-10 000 and (c) MNP-18 000.

phase, forming the crystalline hematite phase at higher temperatures [35].

Fig. 2 shows the XPS spectra for both MNP-MS and MNP-10 000 samples. Fig. 2 (a) displays the XPS spectrum over the entire energy range, where the Fe 2p region (Fe $2p_{1/2}$ and Fe $2p_{3/2}$ at 723.05 eV and 711.40 eV, respectively) and O 1s region (530.50 eV) can be observed. The spectral deconvolution curve of the Fe $2p_{3/2}$ peak (Fig. 2 (b)) reveals the characteristic pattern of magnetite with signals of Fe^{2+} (710 eV) and Fe^{3+} (711.5 eV). The Fe^{2+}/Fe^{3+} ratios were 0.58 for MNP-MS and 0.46

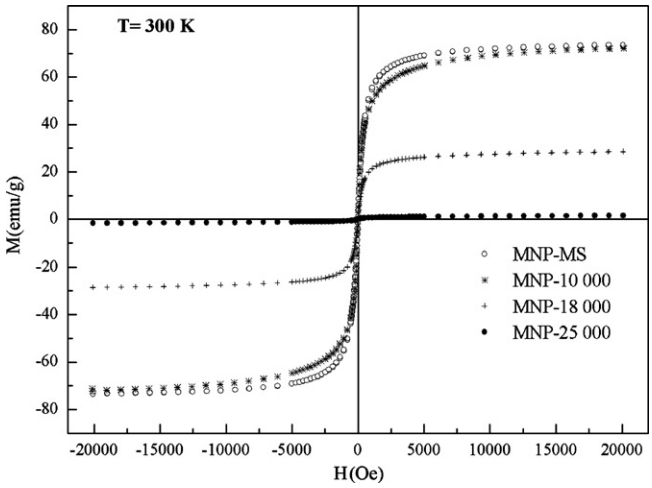

Fig. 4. Hysteresis loops for samples synthesized at different stirring velocities.

for MNP-10 000, both closely to the 0.5 ratio of pure magnetite [36].

The TEM images taken to determine the morphology, shape and size distribution for the particles produced at the different stirring velocities are shown in Fig. 3. The resulting magnetite nanoparticle samples MNP-MS and MS-10 000 are found to be nearly of spherical/ellipsoidal shape (Fig. 3 (a) and (b)). The synthesis using magnetic stirring resulted in nanoparticles with a mean size of ~19 nm and an ample size distribution (Fig. 3 (a)). Interestingly, the magnetite nanoparticles obtained with the homogenizer at 10,000 rpm resulted in a much smaller mean size (10 nm) with a narrow size distribution (Fig. 3 (b)). Even though the shear forces of the mechanical stirring applied with the homogenizer are extremely high and occur in a small space, they cannot be compared to the forces produced by vigorous magnetic stirring [30]. Still, there is no alteration in the nanoparticles' morphological structure: both are spherical/ellipsoidal at 10,000 rpm and for MS. Also the nanoparticles' size distribution is controlled by the nucleus growth process, while diffusion-controlled growth is desired. Improved size distribution can be accomplished by increasing the stirring velocities of the chemicals to speed up the transport of the growth species to the nanoparticle's surface [32]. Fig. 3(c) shows that stirring the solution at 18,000 rpm produced both nanoparticles with different shapes and sizes as well as different sizes of nanorods. Although magnetite nanoparticles possess magnetic axes along the directions (1 1 1) and (1 1 0), providing the possibilities for partial one-dimensional (1D) growth along these magnetic axes [37,38]. Still, they do not grow preferentially by themselves and are mainly restricted by the isotropic spinnel crystal structure and the strong magnetism [39]. The nanorods formed at 18,000 rpm may correspond to partially hydrated goethite nanorods produced via the hydrothermal method described by Qiu et al. [40].

The hydrodynamic diameter of the magnetic samples was measured using DLS. The mean size for the samples MNP-MS and MS-10 000 were 43.8 nm and 29.7 nm, respectively. The mean particle diameter obtained with DLS was about 20 nm larger than the values obtained by TEM. This difference was caused by the aggregation of the magnetic particles, due by the mutual magnetic interaction between them, which disturbed the DLS measurements. The magnetic nanoparticles and nanorods obtained by the co-precipitation method using 18,000 rpm were not suitable for DLS analysis.

The magnetic properties were measured at 300 K for the nanoparticles synthesized at different stirring velocities (Fig. 4). The magnetic curves for the samples MNP-MS and MNP-10 000 shows no hysteresis loop and are reversible at 300 K. No remanence and coercivity were observed for these samples, which is indicative of their superparamagnetic (SPM) behavior. The M_s for MNP-MS (73.2 emu/g) and for MNP-10 000 (72.0 emu/g) are not far from the bulk magnetization value for the magnetite [41]. On the other hand, for sample MNP-18 000, this value reached 28.5 emu/g before decreasing drastically for the sample MNP-25 000. These results are in good agreement with the XRD data for the samples at higher stirring velocities, where other phases of iron compounds are observed. Also, the M_s values obtained for the MNP-MS and MNP-10 000 are higher than those obtained using the co-precipitation method at low temperatures (5 °C) [42] or using NaOH as precipitator [43], although they are lower than those obtained by the inverse co-precipitation method [44].

4. Conclusions

In summary, superparamagnetic nanoparticles of magnetite with a mean diameter of 10 nm and narrow size distribution were synthesized by the co-precipitation method using a homogenizer at a stirring velocity of 10,000 rpm. At this stirring velocity, the mean diameter of the nanoparticles was smaller than the values obtained by vigorous magnetic stirring; they also presented different shapes and morphology form those synthesized with a stirring velocity of 18,000 rpm, which resulted in nanoparticles and nanorods.

The effect of the solution's core temperature is another parameter to take into consideration. An increase in the precursor solution's temperature by high stirring velocities initially promotes the partial thermal oxidation of magnetite to goethite, generating goethite nanorods by the hydrothermal process. If the temperature increase is too great, the final product is a non-magnetic mixture of iron oxide, hematite and goethite instead of magnetite.

Acknowledgements

The financial support for this work was provided by FONDECYT (Grants Nos. 1070492 and 7070109). We greatly appreciate the technical support in the ZetaSizer measurement provided by P.D. Marcato MSc. from IQ-UNICAMP and the XPS analysis by Surface Analysis Laboratory (ASIF), Universidad de Concepción.

R. Valenzuela, student in the Science and Analytical Technology Doctorate Program, thanks the student grants received from the Pharmacy Faculty and Graduate School of the Universidad de Concepción.

S. K. Sharma and M. Knobel are thankful to FAPESP and CNPq (Brazil) for the financial support.

References

[1] A. Garcia, S. Oh, C.R. Engler, Biotechnol. Bioeng. 33 (1989) 321–326.
[2] L.M. Rossi, A.D. Quach, Z. Rosenzweig, Anal. Bioanal. Chem. 380 (2004) 606–613.
[3] B.F. Pan, F. Gao, H.C. Gu, J. Colloid Interface Sci. 284 (2005) 1–6.
[4] Z.F. Gan, J.S. Jiang, Y. Yang, B. Du, M. Qian, P. Zhang, J. Biomed. Mater. Res. Part A 84A (2008) 10–18.
[5] D.-G. Lee, K.M. Ponvel, M. Kim, S. Hwang, I.-S. Ahn, Ch-H. Lee, J. Molec. Catal. B: Enzym 57 (2009) 62–65.
[6] Y.C. Chang, D.H. Chen, J. Colloid Interface Sci. 283 (2005) 446–451.
[7] R.C.C. Costa, F.C.C. Moura, J.D. Ardisson, J.D. Fabris, R.M. Lago, Appl. Catal. B 83 (2008) 131–139.
[8] J. Yang, S.B. Park, H.G. Yoon, Y.M. Huh, S. Haam, Int. J. Pharm. 324 (2006) 185–190.
[9] Y.B. Zhao, Z.M. Qiu, J.Y. Huang, Chin. J. Chem. Eng. 16 (2008) 451–455.
[10] Y. Hirota, Y. Akiyama, Y. Izumi, S. Nishijima, Phys. C 469 (2009) 1853–1856.
[11] L.X. Tiefenauer, A. Tschirky, G. Kuhne, R.Y. Andres, Magn. Reson. Imaging 14 (1996) 391–402.
[12] B. Feng, R.Y. Hong, Y.J. Wu, G.H. Liu, L.H. Zhong, Y. Zheng, J.M. Ding, D.G. Wei, J. Alloys Compd. 473 (2009) 356–362.
[13] A. Jordan, R. Scholz, P. Wust, H. Schirra, T. Schiestel, H. Schmidt, R. Felix, J. Magn. Magn. Mater. 194 (1999) 185–196.
[14] A. Ito, M. Shinkai, H. Honda, T. Kobayashi, J. Biosci. Bioeng. 100 (2005) 1–11.
[15] P. Gould, Nanotoday 1 (2006) 34–39.

[16] M. Mahmoudi, A. Simchi, A.S. Milani, P. Stroeve, J. Colloid Interface Sci. 336 (2009) 510–518.
[17] M. Hnaiein, W.M. Hassen, A. Abdelghani, C. Fournier-Wirth, J. Coste, F. Bessueille, D. Leonard, N. Jaffrezic-Renault, Electrochem. Commun. 10 (2008) 1152–1154.
[18] M. Tada, S. Hatanaka, H. Sanbonsugi, N. Matsushita, M. Abe, J. Appl. Phys. 93 (2003) 7566–7568.
[19] J. Chen, F. Wang, K. Huang, Y. Liu, S. Liu, J. Alloys Compd. 475 (2009) 898–902.
[20] L.S. Darken, R.W. Gurry, J. Am. Chem. Soc. 68 (1946) 798–816.
[21] S. Grimm, T. Stelzner, J. Leuthausser, S. Barth, K. Heide, Thermochim. Acta 300 (1997) 141–148.
[22] K.M. Lee, C.M. Sorensen, K.J. Klabunde, G.C. Hadjipanayis, IEEE Trans. Magn. 28 (1992) 3180–3182.
[23] W. Pei, H. Kumada, T. Natusme, H. Saito, S. Ishio, J. Magn. Magn. Mater. 310 (2006) 2375–2377.
[24] D. Maity, S.N. Kale, R. Kaul-Ghanekar, J.-M. Xue, J. Ding, J. Magn. Magn. Mater. 321 (2009) 3093–3098.
[25] M.H. Liao, D.H. Chen, J. Mater. Chem. 12 (2002) 3654–3659.
[26] T. Feng, Y.M. Du, J.H. Yang, J. Li, X.W. Shi, J. Appl. Polym. Sci. 101 (2006) 1334–1339.
[27] J.P. Jolivet, P. Belleville, E. Tronc, J. Livage, Clays Clay Miner. 40 (1992) 531–539.
[28] D.K. Kim, M. Mikhaylova, Y. Zhang, M. Muhammed, Chem. Mater. 15 (2003) 1617–1627.
[29] K. Tao, H.J. Dou, K. Sun, Colloids Surf. A320 (2008) 115–122.
[30] M. Zlokarnik, Stirring: Theory and Practice, first ed., Wiley-VCH, Weinheim, 2001.
[31] S. Hua, G. Zheng, Y. Zhang, R. Liu, G. Li, J. Dispersion Sci. Technol. 27 (2006) 311–315.
[32] N.K. Devaraj, B.H. Ong, M. Matsumoto, Synth. React. Inorg. Met-Org. Nano-Met. Chem. 38 (2008) 2004–2007.
[33] S. Lian, Z. Khan, E. Wang, M. Jiang, C. Hu, L. Xu, Solid State Commun. 127 (2003) 605–608.
[34] G. Gnanaprakash, S. Mahadevan, T. Jayakumar, P. Kalyanasunduram, J. Philip, B. Raj, Mater. Chem. Phys. 103 (2007) 168–175.
[35] K. Przepiera, A. Przepiera, J. Therm. Anal. Calorim. 65 (2001) 497–503.
[36] T. Missana, C. Maffiotte, M. García-Gutiérrez, J. Colloid Interface Sci. 261 (2003) 154–160.
[37] L. Gu, H. Shen, J. Alloys Compd. 472 (2009) 50–54.
[38] J. Wang, Z. Peng, Y. Huang, Q. Chen, J. Cryst. Growth 276 (2005) 571–576.
[39] X. Lan, X. Cao, W. Qian, W. Gao, C. Zhao, Y. Guo, J. Solid State Chem. 180 (2007) 2340–2345.
[40] X.Q. Qiu, L. Lv, G.-S. Li, W. Han, X.-J. Wang, L.-P. Li, J. Therm. Anal. Calorim. 91 (2008) 873–878.
[41] S. Mohapatra, N. Pramanik, S. Mukherjee, S.K. Ghosh, P. Pramanik, J. Mater. Sci. 42 (2007) 7566–7574.
[42] T. Iwasaki, K. Kosaka, N. Mizutani, S. Watano, T. Yanagida, H. Tanaka, T. Kawai, Mater. Lett. 62 (2008) 4155–4157.
[43] D.L. Zhao, X.W. Zeng, Q.S. Xia, J.T. Tang, J. Alloys Compd. 469 (2009) 215–218.
[44] J. Murbe, A. Rechtenbach, J. Topfer, Mater. Chem. Phys. 110 (2008) 426–433.